Journal of Materials Science: Materials in Electronics
https://doi.org/10.1007/s10854-018-9225-7

A novel low-fired and high-ε_r microwave dielectric ceramic $BaCu(B_2O_5)$-added $0.6Ca_{3/5}La_{4/15}TiO_3–0.4Li_{1/2}Nd_{1/2}TiO_3$

Yong-jun Gu[1,2,3] · **Jin-liang Huang**[1,2] · **Qian Li**[1,2] · **Xiang-mei Ning**[1] · **Li-hua Li**[1] · **Xin-li Li**[2]

Received: 2 March 2018 / Accepted: 2 May 2018

Abstract

A novel low-fired microwave dielectric ceramic, $BaCu(B_2O_5)$-added $0.6Ca_{3/5}La_{4/15}TiO_3–0.4Li_{1/2}Nd_{1/2}TiO_3$ (abbreviated CLT–LNT), was prepared by solid state route. The influence of $BaCu(B_2O_5)$ on the phase composition, sintering behavior and microwave dielectric properties of as-synthesized CLT–LNT ceramics was investigated. All the $BaCu(B_2O_5)$-added CLT–LNT ceramic samples exhibited single phase orthorhombic perovskite structure. $BaCu(B_2O_5)$ dramatically decreased the sintering temperature of CLT–LNT ceramics from 1400 to 930 °C. Favorable microwave dielectric properties ($\varepsilon_r = 87.6$, $Q \times f = 6530$ GHz, $\tau_f = 3.2$ ppm/°C) as well as the maximum relative density (97.9%) were obtained for the 1.6 wt% $BaCu(B_2O_5)$-added CLT–LNT ceramic sintered at 930 °C for 3 h. Therefore, such a novel $BaCu(B_2O_5)$-added CLT–LNT ceramic would be a promising candidate for low-temperature co-fired ceramics applications.

1 Introduction

The past few decades have witnessed tremendous development of wireless communications in cell phone and satellite communication systems. The ever-increasing package density of microwave components, such as filter, oscillator, and antenna, inevitably leads to the rise of chip volume and much generation of heat [1, 2]. To ensure the reliability of components and circuits, thermal conductive filler has been widely used to remove the unwanted heat [3–5]. Ceramics, with large thermal conductivity, could be a better choice. Now, the low-temperature co-fired ceramics (LTCC) technology has become an irreplaceable fabrication approach to realize the miniaturization and integration of microwave circuit system [6]. To meet the requirements of LTCC technology, the dielectrics with high dielectric constant, high quality factor, and near zero temperature coefficient of resonant frequency should be well sintered at low temperature (< 961 °C) to co-fire with Ag [7–9].

However, most of the known commercial ceramic materials with large dielectric constants and high quality factors have high sintering temperatures. To solve this problem, low-melting sintering aids such as oxides, compounds and glass frits are generally mixed with ceramic materials to reduce the sintering temperature. A lot of researchers have made great efforts. Fang et al. lowered the sintering temperature to 950 °C in the $Ca_{0.35}Li_{0.25}Nd_{0.35}Ti_{0.97}Al_{0.03}O_3$ ceramics by adding 5 wt% $BaCu(B_2O_5)$ and obtained the optimized microwave dielectric properties: $\varepsilon_r = 109.5$, $Q \times f = 2979$ GHz, and $\tau_f = 41.2$ ppm/°C [10]. Ren et al. presented a novel LTCC material with sintering temperature of 875 °C based on $CaO–B_2O_3–SiO_2$ glass/$CaTiO_3$ ceramic [11]. This material has the following characteristics: $\varepsilon_r = 25.7$, $Q \times f = 7778$ GHz, $\tau_f = 3.7$ ppm/°C, CTE = 6.9 ppm/K and thermal conductivity $\lambda = 3.4$ W/mK. Zhang et al. investigated the effect of $H_3BO_3–CuO–Li_2CO_3$ combined additives on the sintering temperature of $Ca_{0.61}Nd_{0.26}Ti_{0.98}Sn_{0.02}O_3$ (CNTS) ceramics [12]. The $H_3BO_3–CuO–Li_2CO_3$ combined additives effectively lowered the sintering temperature of CNTS ceramics from 1300 to 950 °C. $Li_{0.5}Nd_{0.5}TiO_3$ (LNT) demonstrated an effective compensation in τ_f value of the low-fired CNTS ceramics. Excellent dielectric properties of $\varepsilon_r = 90.6$, $Q \times f = 3400$ GHz, and $\tau_f = 9$ ppm/°C were

---

✉ Yong-jun Gu
yjgu_ycs@126.com

[1] School of Materials Science and Engineering, Henan University of Science and Technology, Luoyang 471023, China

[2] Collaborative Innovation Center of Nonferrous Metals, Luoyang 471023, Henan, China

[3] Henan Key Laboratory of Materials Science & Processing Technology for Non-ferrous Metals, Luoyang 471023, Henan, China

obtained in the 0.4CNTS–0.6LNT ceramics with 5 wt% (H_3BO_3–CuO)-0.5 wt% Li_2CO_3 sintered at 900 °C for 2 h.

$(1\text{-}x)Ca_{0.6}La_{0.8/3}TiO_3\text{-}xLi_{1/2}Nd_{1/2}TiO_3$ ($0.4 \leq x \leq 0.6$) is a well-known ceramic material for microwave applications due to its high relative permittivity, high quality factor, and near zero temperature coefficient of resonant frequency. Good temperature stability (τ_f = 4.5 ppm/°C) with a high permittivity of 105 and a $Q \times f$ value of 7000 GHz was obtained in the sample sintered at 1400 °C for 4 h when $x = 0.5$ [13]. Meanwhile higher $Q \times f$ value of 7800 GHz with $\tau_f = 51.8$ ppm/°C was also obtained when $x = 0.4$. However, it is difficult to be co-fired with high conductivity electrodes (e.g. Ag) at a low temperature (≤950 °C). According to the previous studies [14, 15], we prepared a novel LTCC material with high permittivity based on $BaCu(B_2O_5)$/CLT–LNT ($0.6Ca_{3/5}La_{4/15}TiO_3$–$0.4Li_{1/2}Nd_{1/2}TiO_3$) ceramic. The sintering temperature, phase composition, microstructure, and microwave dielectric properties were investigated.

2 Experimental procedure

2.1 Materials

All the raw materials, including $CaCO_3$(99%), Li_2CO_3(99%), La_2O_3(99.99%), Nd_2O_3(99.99%), TiO_2(98%), $Ba(OH)_2.8H_2O$(99%), CuO (99%) and H_3BO_3 (99.5%) were obtained from Sinopharm Chemical Reagent Co. Ltd. (Shanghai, China).

2.2 BaCu(B_2O_5) powder preparation

The $BaCu(B_2O_5)$ powder was synthesized by conventional solid-state route. Stoichiometric amounts of $Ba(OH)_2{\cdot}8H_2O$, CuO, and H_3BO_3 were weighed and mixed with ZrO_2 balls in alcohol for 24 h, and then calcined in air at 800 °C for 3 h after being dried at 80 °C. The as-synthesized $BaCu(B_2O_5)$ was crushed, ground, and sieved by 200 mesh.

2.3 CLT–LNT ceramic preparation

Samples of CLT–LNT ceramics were also fabricated by conventional solid-state route. The La_2O_3 and Nd_2O_3 powders were first calcined at 900 °C for 2 h to removal the moisture and CO_2 absorbed from the environment. Stoichiometric amounts of raw powders were weighed according to the formula of CLT–LNT. The powder mixtures were milled with ZrO_2 balls in alcohol for 24 h. The slurry was dried at 80 °C and sieved by 120 mesh screen, and then calcined in air at 1200 °C for 3 h to form the CLT–LNT phase. Then, block CLT–LNT was crushed and milled into fine ceramic powders in high speed (420 r/min) planetary ball mill. The as-synthesized CLT–LNT and $BaCu(B_2O_5)$ powders at different weight ratios (0.4, 0.8, 1.2, 1.6, and 2.0 wt%) were milled for 24 h again, then granulated with PVA binder, and finally uniaxially pressed into cylinders with 10 mm in diameter and 5 mm in height under a pressure of 150 MPa. The cylinders were heated at 600 °C for 2 h to burn out the organic binder at a heating rate of 0.5 °C/min. And then, the pure CLT–LNT and $BuCu(B_2O_5)$-added CLT–LNT pellets were sintered at 1350–1450 °C and at 850–950 °C for 3 h at a heating rate of 5 °C/min, respectively.

2.4 Characterization

The bulk densities of the sintered ceramic samples were measured by the Archimedean immersion method using distilled water as medium with the accuracy of ± 0.001 g/cm^3. The phase composition of the samples were identified by X-ray powder diffraction patterns (XRD, Bruke D8 ADVANCE, Germany, Cu Kα_1, 40 kV and 40 mA). Prior to the examination, the sintered pellets were crushed into powders with an agate mortar. The morphologies of the sintered samples were characterized by scanning electron microscopy (SEM, Jeol, JSM5610LV, Japan). Before visualization, the surfaces of samples were coated with a thin layer of gold to enhance electric conductivity. The quality-factor $Q \times f$ values and the relative dielectric constants ε_r at microwave frequency were determined with a network analyzer (Agilent N5230C, USA) in S_{21} transmission mode at room temperature according to the post-resonant method developed by Hakki and Coleman [16]. The temperature coefficient of the resonant frequency (τ_f) was also measured by the same method at the temperatures ranging from 20 to 80 °C, and calculated by the following equation:

$$\tau_f = \frac{f_{80} - f_{20}}{f_{20} \times (80 - 20)} = \frac{f_{80} - f_{20}}{f_{20} \times 60} \times 10^6 \text{ (ppm/°C)} \quad (1)$$

where f_{80} and f_{20} represent the resonant frequencies at 80 and 20 °C, respectively.

3 Results and discussion

3.1 Phase composition

Figure 1 illustrates the typical room-temperature XRD patterns of the pure CLT–LNT ceramics sintered at 1400 °C for 3 h and the CLT–LNT ceramics with different amount of $BaCu(B_2O_5)$ addition sintered at 930 °C for 3 h. A single orthorhombic perovskite structure without ordered arrangement of cations/vacancies was observed in the as-synthesized CLT–LNT ceramics and complete solid solution of the complex perovskite phase was confirmed (JCPDS78-1013). Meanwhile, the diffraction peak corresponding to the (224)

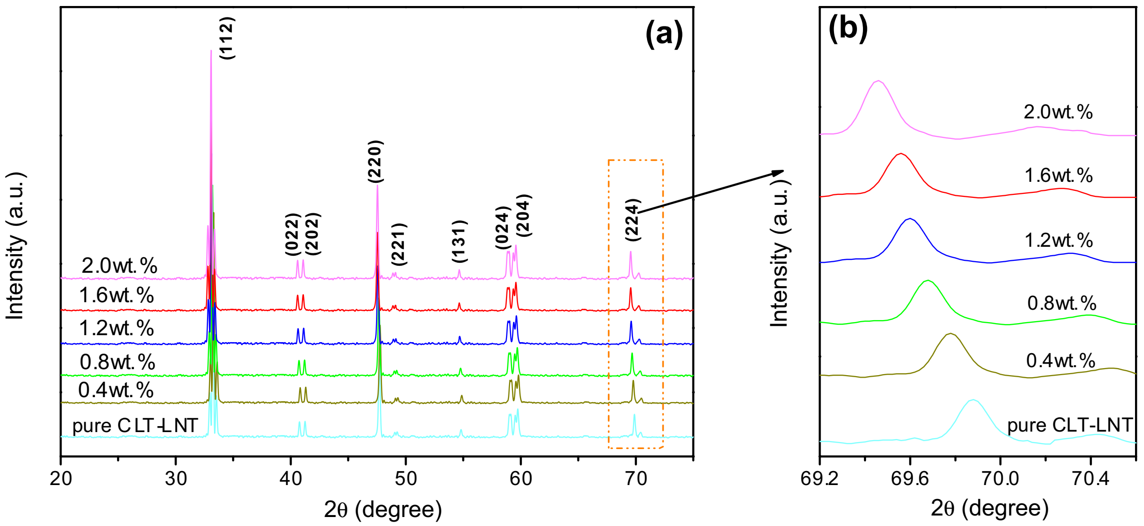

Fig. 1 Typical XRD patterns of the BaCu(B_2O_5)-added CLT–LNT ceramic samples sintered at 930 °C for 3 h and the pure CLT–LNT ceramic sample sintered at 1400 °C for 3 h

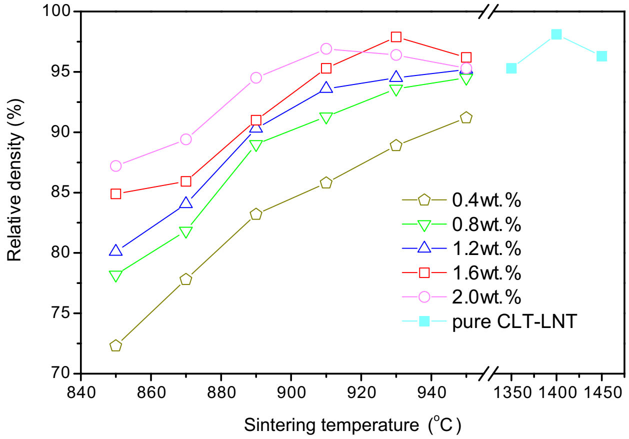

Fig. 2 Relative densities of the BaCu(B_2O_5)-added CLT–LNT ceramic samples sintered at 850–950 °C for 3 h and the pure CLT–LNT ceramic samples sintered 1350–1450 °C for 3 h

crystal face shifted slightly to the low angle with the increment of BaCu(B_2O_5) content, suggesting that the d_{224} value increased with BaCu(B_2O_5) addition according to the Bragg equation (2dsinθ = nλ).

3.2 Sintering behavior

Figure 2 shows the relative densities of the CLT–LNT ceramics with 0.4 ~ 2.0 wt% BaCu(B_2O_5) addition as a function of sintering temperature from 850 to 950 °C and without BaCu(B_2O_5) from 1350 to 1450 °C for 3 h. The relative densities of the BaCu(B_2O_5)-added CLT–LNT ceramics increase initially as the sintering temperatures rise, and then almost saturate at above 930 °C. The relative densities of CLT–LNT ceramics with BaCu(B_2O_5) sintered at 930 °C were almost the same as the pure CLT–LNT ceramic sintered at 1400 °C (98.1% of calculated theoretical density). After adding the BaCu(B_2O_5), the sintering temperature of the CLT–LNT ceramics has been dramatically reduced by 470 °C. The highest relative density (97.9%) could be obtained for the CLT–LNT ceramics with 1.6 wt% BaCu(B_2O_5) sintered at 930 °C. However, further increasing BaCu(B_2O_5) content led to a slight decrease in the relative density.

3.3 Microstructure

Figure 3 illustrated the typical SEM images of the surface morphology of BaCu(B_2O_5)-added CLT–LNT ceramics sintered at 930 °C for 3 h and pure CLT–LNT ceramics sintered at 1300 °C for 3 h. All the specimens except for the 0.4 wt% BaCu(B_2O_5)-added showed dense microstructures with low porosity. It can be seen that a large number of quadrate grains (1–2 μm) existed in BaCu(B_2O_5)-added CLT–LNT ceramics. With the BaCu(B_2O_5) content increasing, the pore volume decreased and the morphology became denser, but there were no significant differences in the number and size of grains. Meanwhile, grains with much larger size (3–5 μm) were observed in the pure CLT–LNT ceramics sintered at 1400 °C for 3 h. This indicated that sintering temperature was the key factor for the grain growth of CLT–LNT ceramic samples other than BaCu(B_2O_5) content.

3.4 Dielectric properties

Figure 4 illustrated the dielectric properties of BaCu(B_2O_5)-added CLT–LNT ceramics sintered at 930 °C for 3 h as a function of BaCu(B_2O_5) content. Clearly, all the BaCu(B_2O_5)

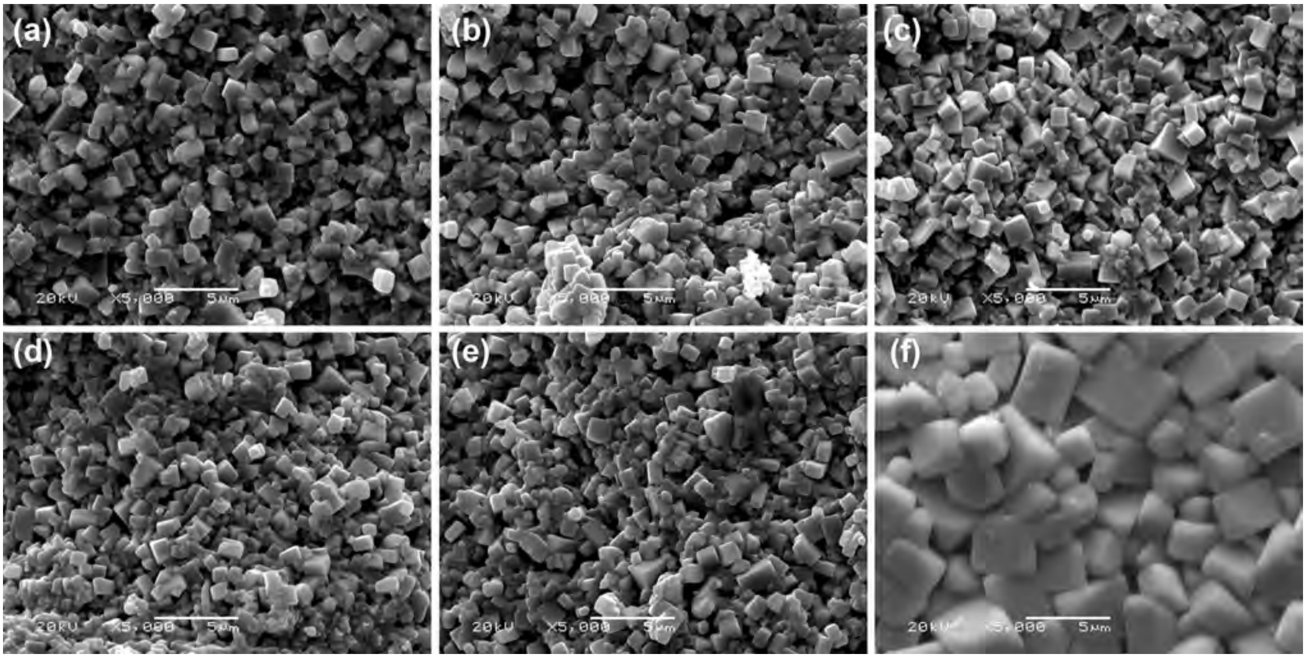

Fig. 3 Typical SEM images of the CLT–LNT ceramics doped by **a** 0.4 wt%, **b** 0.8 wt%, **c** 1.2 wt%, **d** 1.6 wt%, **e** 2.0 wt% BaCu(B_2O_5) sintered at 930 °C for 3 h, and **f** pure CLT–LNT ceramics sintered at 1400 °C for 3 h

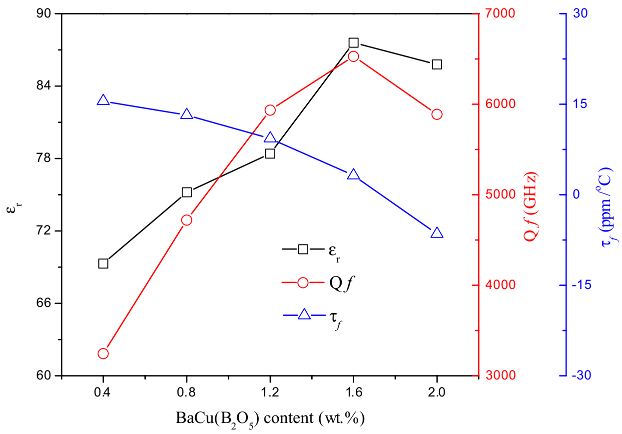

Fig. 4 Dielectric properties (ε_r, Q×f, τ_f) of BaCu(B_2O_5)-added CLT–LNT ceramics sintered at 930 °C for 3 h

added CLT–LNT ceramic samples exhibited lower permittivities than that of pure CLT–LNT ceramic (106) sintered at 1400 °C. This might attribute to low permittivity of the amorphous phase originated from BaCu(B_2O_5) flux during the cooling process. In general, the dielectric constant depends on phase composition, and relative density [17, 18]. In this work, the ε_r values of BaCu(B_2O_5) added CLT–LNT ceramics exhibited the same tendency as the relative densities since higher relative density means lower porosity (ε_r ~ 1) [19]. Therefore, the maximum of ε_r value (87.6) was obtained in well-densified CLT–LNT ceramic sample with 1.6 wt% BaCu(B_2O_5) addition. The Q×f values of BaCu(B_2O_5)-added CLT–LNT ceramic samples increased gradually with the increment of BaCu(B_2O_5) up to 1.6 wt% (the saturated Q×f value is 6530 GHz), and then decreased rapidly for further BaCu(B_2O_5) addition. Generally speaking, the microwave dielectric loss included not only intrinsic losses that were mainly caused by the lattice vibration modes but also extrinsic losses dominated by densification/porosity, the secondary phases, grain sizes and oxygen vacancies, etc. [15, 20–22]. The increasing of the ε_r and $Q \times f$ value with the increment of BaCu(B_2O_5) contents should be attributed to the improved densification. Another explanation might be the restrained evaporation of lithium during the sintering process at 930 °C, much lower than the sintering temperature of pure CLT–LNT ceramic. It was also clearly observed that the temperature coefficient of the resonant frequency (τ_f) decreased slightly with the BaCu(B_2O_5) content, from 15.5 to − 6.5 ppm/°C, due to the negative τ_f value of BaCu(B_2O_5) (− 32 ppm/°C) [23, 24]. In summary, BaCu(B_2O_5) dramatically decreased the sintering temperature of the CLT–LNT ceramic while causing not that much deterioration in microwave dielectric properties. The optimum microwave dielectric properties of $\varepsilon_r = 87.6$, Q×f = 6530 GHz, and $\tau_f = 3.2$ ppm/°C were obtained for 1.6 wt% BaCu(B_2O_5)-added CLT–LNT ceramics sintered at 930 °C for 3 h.

As known, the temperature coefficient of resonant frequency (τ_f) was a critical factor for the microwave component, especially for the wireless communication applications, and a near zero τ_f value was often expected [25]. Moreover, high quality factor was also required to ensure the selection of desired signal and the removal of unwanted ones by its narrow bandwidth and a relatively high dielectric constant for minimization of the component [26]. Figure 5 showed the microwave dielectric properties of CaO–Li$_2$O–Re$_2$O$_3$–TiO$_2$ based ceramics and some typical low temperature sintered ceramics with $\varepsilon_r \geq 70$. It was clearly seen that only twelve ceramics met the requirement of sintering temperature to be lower than 961 °C. Considering that the near zero temperature coefficient of resonant frequency ($|\tau_f| < 10$ ppm/°C) was required, the BaCu(B$_2$O$_5$)-added CLT–LNT ceramics in this work possessed much higher Q × *f* and relative permittivity values.

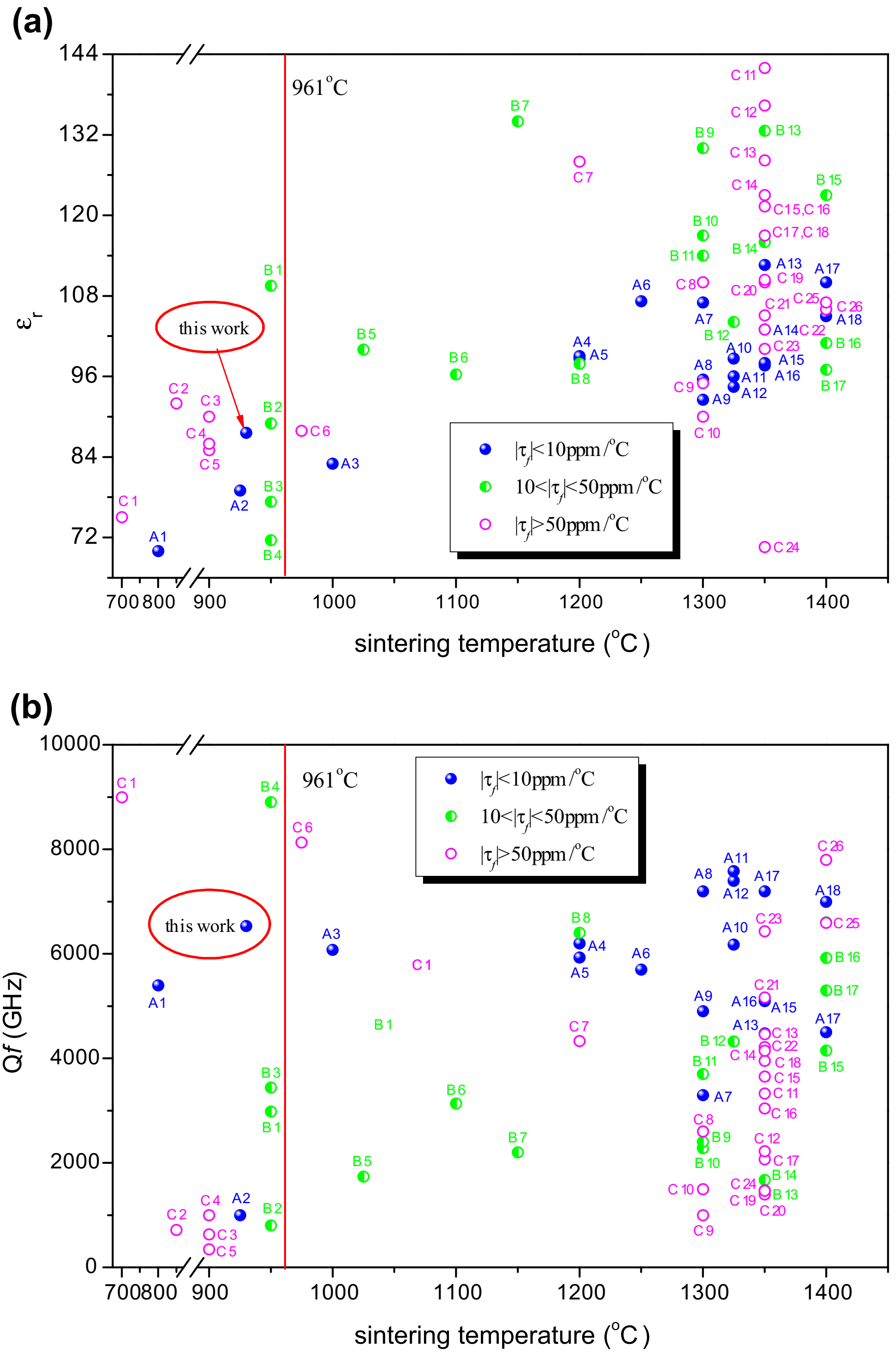

Fig. 5 Microwave dielectric properties of CaO–Li$_2$O–Re$_2$O$_3$–TiO$_2$ based ceramics (Re = rare earth) and some typical low temperature sintered ceramics with relative permittivity over 70. **a** permittivity (ε_r), **b** Q × *f*. *A1* (after Ref. [27]); *A2* (after Ref. [28]); *A3* (after Ref. [29]); *A4* (after Ref. [30, 31]); *A5* (after Ref. [32]); *A6* (after Ref. [33]); *A7, A9* (after Ref. [34]); *A8* (after Ref. [35]); *A10, A12, B12* (after Ref. [36]); *A11, A14, B16* (after Ref. [37]); *A13* (after Ref. [38]); *A15, A16, B13, B14, C11–C24* (after Ref. [39]); *A17, B12* (after Ref. [40]); *A18, C26* (after Ref. [13]); *B1, C7* (after Ref. [10]); *B2* (after Ref. [41]); *B3* (after Ref. [42]); *B4* (after Ref. [15]); *B5* (after Ref. [43]); *B6* (after Ref. [44]); *B7* (after Ref. [45]); *B8* (after Ref. [46]); *B9* (after Ref. [47]); *B10* (after Ref. [48]); *B11* (after Ref. [49]); *B15* (after Ref. [50]); *B17, C25* (after Ref. [51]); *C1* (after Ref. [52]); *C2–C5* (after Ref. [53]); *C6* (after Ref. [54]); *C8* (after Ref. [55]); *C9, C10* (after Ref. [56]). Red line inserted in the figure shows the melt point of silver

4 Conclusions

A novel low-fired and high-ε_r microwave dielectric ceramic $BaCu(B_2O_5)$-added CLT–LNT was fabricated, and the sintering behaviors and microwave dielectric properties of the CLT–LNT ceramics with different amounts of $BaCu(B_2O_5)$ addition had been investigated. $BaCu(B_2O_5)$ lowered the sintering temperature of CLT–LNT ceramics from 1400 to 930 °C and improved its densification. No second phase was detected in all the $BaCu(B_2O_5)$-added CLT–LNT ceramic samples. The 1.6 wt% $BaCu(B_2O_5)$-added CLT–LNT ceramics sintered at 930 °C for 3 h had optimum microwave dielectric properties of $\varepsilon_r = 87.6$, $Q \times f = 6530$ GHz, and $\tau_f = 3.2$ ppm/°C, enabling it a promising material for LTCC applications.

Acknowledgements This work was supported by the Natural Science Foundation of Henan Province (162300410088) and Development Funds of Henan University of Science & Technology for High Level Scientific Research Project (2015GJB005).

References

1. G. Wu, Y. Wang, K. Wang, A. Feng, RSC Adv. **6**, 102542 (2016)
2. C. Pan, J. Zhang, K. Kou, Y. Zhang, G. Wu, Int. J. Heat Mass Transf. **120**, 1 (2018)
3. A. Feng, G. Wu, C. Pan, Y. Wang, J. Nanosci. Nanotechnol. **17**, 3786 (2017)
4. Y. Wang, W. Zhang, X. Wu, C. Luo, Q. Wang, J. Li, L. Hu, Synth. Met. **228**, 18 (2017)
5. A. Feng, Z. Jia, Q. Yu, H. Zhang, G. Wu, Nano **13**, 1850037 (2018)
6. R. Zuo, J. Zhang, J. Song, Y. Xu, J. Am. Ceram. Soc. **101**, 569 (2018)
7. H. Yang, B. Tang, Z. Fang, J. Luo, S. Zhang, J. Am. Ceram. Soc. **101**, 2202 (2018)
8. Z. Wang, R. Freer, J. Eur. Ceram. Soc. **35**, 3033 (2015)
9. C.F. Tseng, P.J. Tseng, C.M. Chang, Y.C. Kao, J. Am. Ceram. Soc. **97**, 1918 (2014)
10. Z.X. Fang, B. Tang, F. Si, S.R. Zhang, J. Alloy Compd. **693**, 843 (2017)
11. L. Ren, X. Luo, L. Hu, Q. Sun, Y. Xia, Y. Hu, W. Gong, H. Zhou, J. Eur. Ceram. Soc. **37**, 619 (2017)
12. Q.L. Zhang, H.P. Sun, H. Yang, J. Alloy Compd. **509**, 9986 (2011)
13. C.L. Huang, J.T. Tsai, Y.B. Chen, Mater. Res. Bull. **36**, 547 (2001)
14. Y.J. Gu, C. Li, J.L. Huang, Q. Li, L.H. Li, X.L. Li, J. Eur. Ceram. Soc. **37**, 4673 (2017)
15. F.F. Gu, G.H. Chen, C.L. Yuan, C.R. Zhou, T. Yang, Y. Yang, Mater. Res. Bull. **61**, 245 (2015)
16. B.W. Hakki, P.D. Coleman, IEEE Trans. Microw. Theory Tech. **8**, 402 (1960)
17. R. Freer, F. Azough, J. Eur. Ceram. Soc. **28**, 1433 (2008)
18. S. Peng, J. Xu, H. Li, T. Huang, S. Wang, B. Xie, G. Luo, J. Zhou, J. Mater. Sci.: Mater. Electron. **26**, 8819 (2015)
19. M.H. Kim, J.B. Lim, S. Nahm, J.H. Paik, H.J. Lee, J. Eur. Ceram. Soc. **27**, 3033 (2007)
20. H.F. Zhou, N. Wang, X.H. Tan, J. Huang, X.L. Chen, J. Mater. Sci.: Mater. Electron. **27**, 11850 (2016)
21. X. Tang, H. Yang, Q.L. Zhang, J.H. Zhou, Ceram. Int. **40**, 12875 (2014)
22. D. Zhou, G. Dou, M. Guo, S. Gong, Mater. Chem. Phys. **130**, 903 (2011)
23. J. Li, B. Yao, D. Xu, Z. Huang, Z. Wang, X. Wu, C. Fan, J. Alloy Compd. **663**, 494 (2016)
24. M.H. Kim, J.B. Lim, J.C. Kim, S. Nahm, J.H. Paik, J.H. Kim, K.S. Park, J. Am. Ceram. Soc. **89**, 3124 (2006)
25. H. Hughes, F. Azough, R. Freer, D. Iddles, J. Eur. Ceram. Soc. **25**, 2755 (2005)
26. H. Yu, J. Liu, W. Zhang, S. Zhang, J. Mater. Sci.: Mater. Electron. **26**, 9414 (2015)
27. Q. Zeng, W. Li, J.L. Shi, J.K. Guo, H. Chen, M.L. Liu, J. Eur. Ceram. Soc. **27**, 261 (2007)
28. K. Hiroshi, I. Tatsuya, K. Junichi, K. Ichirou, Jpn. J. Appl. Phys. **31**, 3152 (1992)
29. J.Y. Ha, J.W. Choi, H.J. Kim, S.J. Yoon, K.H. Yoon, Mater. Chem. Phys. **79**, 261 (2003)
30. W.S. Kim, K.H. Yoon, E.S. Kim, Jpn. J. Appl. Phys. **39**, 5650 (2000)
31. G.H. Huang, D.X. Zhou, J.M. Xu, Z.P. Zheng, S.P. Gong, Mater. Res. Bull. **40**, 13 (2005)
32. K.H. Yoon, M.S. Park, J.Y. Cho, E.S. Kim, J. Eur. Ceram. Soc. **23**, 2423 (2003)
33. M.T. Sebastian, *Dielectric Materials for Wireless Communication*, 1st edn. (Elsevier, Oxford, 2008), pp. 611–611
34. W.S. Kim, E.S. Kim, K.H. Yoon, Ferroelectrics **223**, 277 (1999)
35. K.H. Yoon, Y.H. Chang, W.S. Kim, J.B. Kim, E.S. Kim, Jpn. J. Appl. Phys. **35**, 5145 (1996)
36. Y.C. Chen, P.S. Cheng, C.F. Yang, W.C. Tzou, J. Mater. Sci. Lett. **20**, 863 (2001)
37. C.L. Huang, J.T. Tsai, J.L. Li, J. Mater. Sci. **35**, 4901 (2000)
38. T. Liu, X.Z. Zhao, W. Chen, J. Am. Ceram. Soc. **89**, 1153 (2006)
39. J.S. Kim, C.I. Cheon, H.J. Kang, C.H. Lee, K.Y. Kim, S. Nam, J.D. Byun, Jpn. J. Appl. Phys. **38**, 5633 (1999)
40. K. Ezaki, Y. Baba, H. Takahashi, K. Shibata, S. Nakano, Jpn. J. Appl. Phys. **32**, 4319 (1993)
41. C. Qin, Z. Yue, Z. Gui, L. Li, Mater. Sci. Eng. B **99**, 286 (2003)
42. Y. Ota, K. Kakimoto, H. Ohsato, T. Okawa, J. Eur. Ceram. Soc. **24**, 1755 (2004)
43. C. Yuan, G. Chen, T. Yang, F. Liu, C. Zhou, Y. Yang, J. Electron. Mater. **44**, 263 (2015)
44. G.H. Chen, C.L. Yuan, C.R. Zhou, Y. Yang, Ceram. Int. **39**, 9763 (2013)
45. E.S. Kim, B.S. Chun, D.W. Yoo, K.H. Yoon, Mater. Sci. Eng. B **99**, 247 (2003)
46. K.H. Yoon, M.S. Park, E.S. Kim, Ferroelectrics **262**, 1147 (2001)
47. T. Lowe, F. Azough, R. Freer, J. Electroceram. **16**, 257 (2006)
48. N. Ichinose, K. Mutoh, J. Eur. Ceram. Soc. **23**, 2455 (2003)
49. E.S. Kim, K.H. Yoon, J. Eur. Ceram. Soc. **23**, 2397 (2003)
50. H. Takahashi, Y. Baba, K. Ezaki, K. Shibata, Jpn. J. Appl. Phys. **35**, 5069 (1996)
51. H.L. Chen, C.L. Huang, Jpn. J. Appl. Phys. **41**, 5650 (2002)
52. D. Zhou, L.X. Pang, Z.M. Qi, Inorg. Chem. **53**, 9222 (2014)
53. P. Samoukhina, S. Kamba, S. Santhi, J. Petzelt, M. Valant, D. Suvorov, J. Eur. Ceram. Soc. **25**, 3085 (2005)
54. E.Z. Li, N. Niu, S.X. Duan, Y. Yuan, B. Tang, J. Mater. Sci.: Mater. Electron. **27**, 3164 (2016)
55. D.A. Abdel Aziz, I. Sterianou, I.M. Reaney, J. Mater. Sci. **44**, 6247 (2009)
56. A.G. Belous, O.V. Ovchar, J. Eur. Ceram. Soc. **23**, 2525 (2003)